Bit error probability approximation for short-time Fourier transform based nonstationary interference excision in DS-SS systems

Slobodan Djukanović, Miloš Daković, LJubiša Stanković

Abstract— **The problem addressed in this paper is bit error probability (BEP) approximation in direct sequence spread-spectrum (DS-SS) systems that implement the short-time Fourier transform (STFT) as a means of nonstationary jammer excision. The jammer, previously concentrated in the time-frequency (t-f) plane, is suppressed by removing its t-f signature via a binary mask. The applied binary mask gives rise to odd higher-order central moments of the decision variable d, i.e., introduces a deviation in the probability density function of d, $f_d(x)$, from a Gaussian law. Two analytical approximations to $f_d(x)$ are proposed, Gaussian approximation (GA) and Hermite-Gaussian approximation (HGA). The HGA takes advantage of the Hermite polynomials and central moments of d thus reducing approximation error introduced by the GA. Analytical expressions for the mean, variance and third central moment of d, when the STFT of the received signal is modified by an arbitrary two-dimensional function, are derived and numerically confirmed. The HGA outperforms the GA for various types of monocomponent and multicomponent jammers, which was verified by simulations.**

I. Introduction

Numerous methods for nonstationary jammer suppression in direct sequence spread-spectrum (DS-SS) systems have been proposed in the literature. In particular, it is shown that time-frequency (t-f) based methods effectively enhance the performance of DS-SS receiver when the received SS signal is corrupted by broadband interferences characterized by narrowband instantaneous bandwidths [1]. Linear t-f methods [2] can filter a corrupted SS signal in the transform domain, with corresponding reconstruction (synthesis) procedure outputting the jammer-free received signal. Proposed linear t-f methods include the well-known short-time Fourier transform (STFT) [3], the fractional Fourier transform (FRFT) [4] and the local polynomial Fourier transform (LPFT) [5], [6]. In these papers, the jammer removal is performed in the transform domain via a binary mask, which excises frequency bins of the representation corrupted by jammer.

However, the problem of bit error probability (BEP) calculation, or approximation, has not been treated in [3]-[6]. This paper addresses the problem of BEP approximation in DS-SS systems that implement the STFT as a means of jammer suppression, which is equivalent to the problem of modelling the decision variable d output by the receiver correlator. When no modification is made in the t-f domain, the decision variable can be well approximated by a Gaussian one according to the central limit theorem (CLT). Nonetheless, by modifying the STFT, the binary mask gives rise to odd higher-order central moments of d, implying that its probability density function (p.d.f.) deviates from the Gaussian law.

Two analytical approximations to the BEP are herein proposed, Gaussian approximation (GA) and Hermite-Gaussian approximation (HGA). The former models the decision variable as a Gaussian one, whereas the latter uses the Hermite polynomials and the third central moment of the decision variable to reduce the approximation error introduced by the former.

Paper is organized as follows. Section 2 briefly describes the STFT based filtering and simple synthesis procedure. The mean, vari-

Signal Processing, Vol. 89, No. 11, Nov. 2009.

ance and third central moment of the decision variable are analytically derived in Section 3, showing their dependence on the applied binary excision mask. In addition, two BEP approximations are introduced. Performance of the proposed approximations is assessed in Section 4 by means of simulations carried out on the received signal corrupted by various FM jammer types, both monocomponent and multicomponent. Conclusions are drawn in Section 5.

II. STFT BASED JAMMER EXCISION IN DS-SS SYSTEMS

The basics of DS-SS systems can be found in [5] and [10]. The N-samples long baseband received signal $x(n)$ is composed of three sequences as follows [3], [6], [10]:

$$x(n) = s(n) + j(n) + \xi(n), \quad n = 1, 2, ..., N \tag{1}$$

where $s(n)$ is an SS sequence of unit amplitude, $j(n)$ is a jammer sequence and $\xi(n)$ is an additive white Gaussian noise (AWGN) sequence with zero mean and variance σ_ξ^2. All the three sequences are uncorrelated with each other. The jammer can be analytically expressed as [6]

$$j(n) = a_j \cos(\varphi(n)) \tag{2}$$

where $\varphi(n)$ and a_j respectively represent its phase and amplitude. For the unit-amplitude SS signal, signal-to-noise ratio (SNR) and jammer-to-signal ratio (JSR) are defined as

$$\text{SNR} = -10\log_{10}\left(\sigma_\xi^2\right) \tag{3}$$

$$\text{JSR} = 10\log_{10}\left(a_j^2/2\right). \tag{4}$$

In addition, the SS signal with one sample per chip is herein assumed, when the perfectly flat spectrum is obtained [8]. Therefore, $s(n)$ equals $p(n)$ or $-p(n)$, depending on a transmitted bit value, and $p(n)$ is a pseudo-noise (PN) sequence, known to both transmitter and receiver. The PN sequence is characterized by the length L and $E[p(n)] = 0$ and $E[p(n)\,p(m)] = \delta(n-m)$, where $E[\cdot]$ denotes the statistical expectation and $\delta(n)$ is the Dirac delta function. Without loss of generality, we will herein adopt an odd value for L.

The STFT of the signal $x(n)$, $X(n,k)$, is given by [3], [6]

$$X(n,k) = \sum_{m=-\frac{N-1}{2}}^{\frac{N-1}{2}} x(n+m)\, w(m)\, e^{-j\frac{2\pi}{N}mk}, \tag{5}$$

where $w(m)$ is a real symmetric analysis window and N is the number of frequency bins. It is also assumed that $N = L$ [3], [6], [8]. Given $w(0) = 1$, a simple manipulation of (5) gives the STFT synthesis equation [6]

$$x(n) = \frac{1}{N}\sum_{k=0}^{N-1} X(n,k). \tag{6}$$

Note that this synthesis requires one summation less than the overlap-add (OLA) method used in [3].

The jammer excision is performed in the t-f plane by removing its t-f signature via binary mask $B(n,k)$, which is the function defined as

$$B(n,k) = \begin{cases} 0, & X(n,k) \text{ contains a jammer} \\ 1, & X(n,k) \text{ otherwise.} \end{cases} \tag{7}$$

Decision whether $X(n,k)$ contains a jammer or not is made by comparing $|X(n,k)|$ to preset threshold value [3]. The synthesis is then performed on the masked STFT to recover the jammer-free received signal $x'(n)$ as follows:

$$x'(n) = \frac{1}{N}\sum_{k=0}^{N-1} X(n,k)\, B(n,k). \tag{8}$$

One realization of $|X(n,k)|$ for the received signal $x(n)$ corrupted by a linear FM modulated (chirp) jammer is depicted in Fig. 1(a), and the binary mask that excises this jammer is shown in Fig. 1(b).

In the STFT calculation, the problem of jammer concentration in the t-f plane also has to be addressed. Namely, the higher the jammer concentration the lesser the excised area, and, taking this into consideration, the window length will be calculated according to the following concentration measure [3], [7]:

$$v = \frac{\sum_{n=1}^{N}\sum_{k=0}^{N-1} |X(n,k)|^4}{\left(\sum_{n=1}^{N}\sum_{k=0}^{N-1} |X(n,k)|^2\right)^2} \tag{9}$$

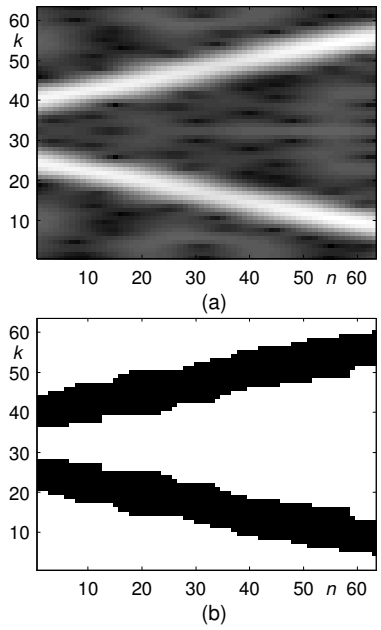

Fig. 1. (a) The STFT of the received signal corrupted by a linear FM jammer. The clearest gray tones of the color-map correspond to the strongest frequency components. (b) Binary mask that excises corrupted frequency components (zero values are shown in black).

so that the jammer is optimally concentrated in the t-f plane. The ratio v favors "peaky" distributions and its highest value corresponds to the best t-f concentration [3].

III. Bit error probability approximations

The decision variable d, output by the receiver correlator and used for the information symbol detection, is given by [3]

$$d = \sum\nolimits_{n=1}^{N} x'(n)\, p(n). \tag{10}$$

Since we are interested only in the real part of d, hereafter we will use

$$d = \mathrm{Re}\left[\sum\nolimits_{n=1}^{N} x'(n)\, p(n)\right]. \tag{11}$$

The output signal-to-noise ratio, SNR_{out}, is defined by [1]

$$\mathrm{SNR}_{out} = \frac{E^2[d]}{\mathrm{Var}[d]} \tag{12}$$

where Var[·] represents the variance operator.

If the STFT is not modified by the binary mask (i.e., no jammer excision is performed), then $x'(n) = x(n)$ and, according to the CLT, d can be modelled by a Gaussian variable with the mean $\mu = N$ and variance $\sigma^2 = N(a_j^2/2 + \sigma_\xi^2)$, assuming that bit "+1" is transmitted. Therefore, in this case, the exact value of the BEP, denoted as P_e, equals [13]

$$P_e = \frac{1}{\sqrt{2\pi}} \int_{\frac{\mu}{\sigma}}^{\infty} e^{-t^2/2} dt = Q\left(\frac{\mu}{\sigma}\right) \tag{13}$$

where

$$Q(x) = \frac{1}{\sqrt{2\pi}} \int_{x}^{\infty} e^{-t^2/2} dt.$$

Nevertheless, if the STFT is modified by the jammer excision binary mask, the synthesized PN sequence will no longer coincide with the original one, implying that (13) cannot be further used for the exact BEP calculation.

Generally, the BEP equals

$$P_e = \int_{-\infty}^{0} f_d(x)\, dx \tag{14}$$

where $f_d(x)$ denotes the p.d.f. of d. Due to excessive complexity of analytical determination of $f_d(x)$, we must resort to its approximations.

The first adopted BEP approximation is a Gaussian approximation, whose p.d.f. is denoted as $f_{\mathrm{GA}}(x)$. The GA outputs results according to (13), and its parameters, the mean μ and the variance σ^2, depend on the applied binary mask and will be derived afterwards.

The accuracy of the GA can be additionally improved by using the central moments $\mu_n = E[(d-\mu)^n]$ of d and the Hermite polynomials, defined by [9], [12]

$$H_k(x) = (-1)^k e^{x^2/2} \frac{d^k}{dx^k} e^{-x^2/2}. \tag{15}$$

Since these polynomials form a complete orthogonal set on the real line, an approximation error $\varepsilon(x)$ introduced by the GA can be

expressed as a series

$$\begin{aligned}\varepsilon(x) &= f_d(x) - f_{\mathrm{GA}}(x) \\ &= f_d(x) - \frac{1}{\sigma\sqrt{2\pi}} e^{-\frac{(x-\mu)^2}{2\sigma^2}} \\ &= \frac{1}{\sigma\sqrt{2\pi}} e^{-\frac{(x-\mu)^2}{2\sigma^2}} \sum_{k=3}^{\infty} C_k H_k\left(\frac{x-\mu}{\sigma}\right). \quad (16)\end{aligned}$$

The series starts with $k = 3$ because the central moments of $\varepsilon(x)$ of order less than 3 are 0 [12]. The coefficients C_k can be expressed in terms of μ_n. In particular, the following relations hold [12, p. 217]:

$$3!\sigma^3 C_3 = \mu_3 \quad (17)$$

$$4!\sigma^4 C_4 = \mu_4 - 3\sigma^4. \quad (18)$$

Due to the complexity of the calculation of C_k (see (28)), only the first-order correction of $f_{\mathrm{GA}}(x)$ will be determined herein. This approximation will be referred to as a Hermite-Gaussian approximation, with the p.d.f. $f_{\mathrm{HGA}}(x)$. Since $H_3(x) = x^3 - 3x$, one obtains [12]

$$\begin{aligned}f_{\mathrm{HGA}}(x) &= \frac{1}{\sigma\sqrt{2\pi}} e^{-\frac{(x-\mu)^2}{2\sigma^2}} \\ &\times \left[1 + \frac{\mu_3}{6\sigma^3}\left(\frac{(x-\mu)^3}{\sigma^3} - \frac{3(x-\mu)}{\sigma}\right)\right]. \quad (19)\end{aligned}$$

Alternatively, $f_{\mathrm{HGA}}(x)$ can be obtained by including only the first correction term to the normal distribution in the Gram-Charlier series [13].

The determination of $f_{\mathrm{GA}}(x)$ and $f_{\mathrm{HGA}}(x)$ entails finding the mean, variance and third central moment of the decision variable d. Assuming that bit "+1" is transmitted and by substituting (5) and (8) into (11), d becomes

$$\begin{aligned}d = \frac{1}{N}\sum_{n=1}^{N}\sum_{k=0}^{N-1}\sum_{m=-\frac{N-1}{2}}^{\frac{N-1}{2}} &[p(m+n) + \xi(m+n)] \\ &\times p(n)\, w(m)\, B(n,k)\cos(\frac{2\pi}{N}mk). \quad (20)\end{aligned}$$

We have made the assumption that the residual jammer can be neglected in the analysis[1] [3], [6], and therefore only the PN and AWGN components are considered in the previous equation. The mean of d is simply obtained from (20) as

$$\mu = E[d] = \frac{1}{N}\sum_{n=1}^{N}\sum_{k=0}^{N-1} B(n,k). \quad (21)$$

The variance of d is, by definition, $\sigma^2 = E[d^2] - \mu^2$, and we proceed with the calculation of $E[d^2]$. By using (20), we get

$$\begin{aligned}E\left[d^2\right] = \frac{1}{N^2}&\sum_{n_1,n_2}\sum_{k_1,k_2}\sum_{m_1,m_2} w(m_1)\, w(m_2) \\ &\times B(n_1,k_1)\, B(n_2,k_2) \\ &\times \cos(\frac{2\pi}{N}m_1k_1)\cos(\frac{2\pi}{N}m_2k_2) \\ &\times E\left[p(m_1+n_1)\, p(n_1)\, p(m_2+n_2)\, p(n_2)\right] \\ &+ \frac{\sigma_\xi^2}{N^2}\sum_{n_1,n_2}\sum_{k_1,k_2}\sum_{m_1,m_2} w(m_1)\, w(m_2) \\ &\times B(n_1,k_1)\, B(n_2,k_2) \\ &\times \cos(\frac{2\pi}{N}m_1k_1)\cos(\frac{2\pi}{N}m_2k_2) \\ &\times \delta(n_1-n_2)\,\delta(m_1-m_2)\end{aligned} \quad (22)$$

where n_1 and n_2 run from 1 to N, k_1 and k_2 run from 0 to $N-1$, whereas m_1 and m_2 run from $-(N-1)/2$ to $(N-1)/2$. As (22) indicates, $E[d^2]$ comprises two components, and for the calculation of the first one we will use the following identity [3], [6]:

$$\begin{aligned}E\left[p(i)\, p(j)\, p(k)\, p(l)\right] &= \delta(i-j)\,\delta(k-l) \\ &+ \delta(i-l)\,\delta(j-k) + \delta(i-k)\,\delta(j-l) \\ &- 2\delta(i-j)\,\delta(k-l)\,\delta(i-k). \quad (23)\end{aligned}$$

[1] As a matter of fact, the jammer component cannot be completely removed from the t-f plane without completely removing other components. This is a consequence of the spectral leakage effect caused by a finite length of the analysis window. However, for a given time instant, one can neglect a portion of the jammer power concentrated in sidelobes of its spectrum, especially when windows characterized by highly suppressed sidelobes are used (e.g., Kaiser or Blackman window). These windows attain the high sidelobes suppression at the expense of the width of the main lobe. Therefore, in this paper, only such windows will be considered, and to completely remove the jammer means to excise only its main lobe.

Let us briefly explain the previous identity. Since $p(n)$ takes on values $+1$ and -1 with equal probability [11], $E[p(i)p(j)p(k)p(l)]$ will be non-zero (i.e., will equal 1) only when the indices i, j, k and l are equal in pairs (first 3 components in (23)). The fourth component is introduced so as to compensate the contribution of the first 3 components when all the indices coincide.

The straightforward calculation yields the final form for σ^2

$$\begin{aligned}\sigma^2 =& \sum_m w^2(m) \sum_n b_n(m) \\ & \times \left[b_{n+m}(m) + (1+\sigma_\xi^2) b_n(m)\right] \\ & - 2\sum_n b_n^2(0)\end{aligned} \tag{24}$$

where

$$b_n(m) = \frac{1}{N}\sum_{k=0}^{N-1} B(n,k)\cos(\frac{2\pi}{N}mk) \tag{25}$$

with m and n running within the above defined limits. Alternatively, σ^2 can be expressed as follows:

$$\sigma^2 = \langle \mathbf{x_1}, \mathbf{w_1}\rangle - 2\left\|\mathbf{x_2}\right\|^2 \tag{26}$$

where $\langle \mathbf{x}, \mathbf{y}\rangle$ represents the inner product of vectors $\mathbf{x}$ and $\mathbf{y}$ (or matrices $\mathbf{x}$ and $\mathbf{y}$, when it represents the Frobenius inner product), $\|\mathbf{x}\|$ represents the Euclidean norm of vector $\mathbf{x}$ (that is, $\|\mathbf{x}\| = \sqrt{\langle \mathbf{x}, \mathbf{x}\rangle}$), $\mathbf{x_1}$ is the $1 \times N$ vector with

$$x_1(m) = \sum_n b_n(m)\left[b_{n+m}(m) + (1+\sigma_\xi^2) b_n(m)\right]$$

and $\mathbf{w_1}$ and $\mathbf{x_2}$ are the $1 \times N$ vectors defined by

$$\begin{aligned}\mathbf{w_1} &= [w^2(-\frac{N-1}{2}), w^2(-\frac{N-3}{2}), \cdots, w^2(\frac{N-1}{2})] \\ \mathbf{x_2} &= [b_1(0), b_2(0), \cdots, b_N(0)].\end{aligned}$$

Knowing the mean (21) and the variance (24) of the decision variable, the exact SNR_{out} value (12) can be calculated for any applied binary mask $\mathbf{B}$.

The third central moment of d is, by definition, $\mu_3 = E[(d-\mu)^3] = E[d^3] - 3\mu E[d^2] + 2\mu^3$. Since the last two components have already been calculated, attention will be focused on $E[d^3]$. By using (20), we get

$$\begin{aligned}E\left[d^3\right] =& \frac{1}{N^3} \\ & \times \sum_{n_{1,2,3}} \sum_{k_{1,2,3}} \sum_{m_{1,2,3}} w(m_1)w(m_2)w(m_3) \\ & \times B(n_1,k_1)B(n_2,k_2)B(n_3,k_3) \\ & \times \cos(\frac{2\pi}{N}m_1k_1)\cos(\frac{2\pi}{N}m_2k_2)\cos(\frac{2\pi}{N}m_3k_3) \\ & \times E[p(m_1+n_1)p(n_1)p(m_2+n_2) \\ & \times p(n_2)p(m_3+n_3)p(n_3)] \\ & + \frac{3\sigma_\xi^2}{N^3} \sum_{n_{1,2,3}} \sum_{k_{1,2,3}} \sum_{m_{1,2,3}} w(m_1)w(m_2)w(m_3) \\ & \times B(n_1,k_1)B(n_2,k_2)B(n_3,k_3) \\ & \times \cos(\frac{2\pi}{N}m_1k_1)\cos(\frac{2\pi}{N}m_2k_2)\cos(\frac{2\pi}{N}m_3k_3) \\ & \times \delta(m_2+n_2-m_3-n_3) \\ & \times E[p(n_1)p(n_2)p(n_3)p(m_1+n_1)]\end{aligned} \tag{27}$$

where $\sum_{n_{1,2,3}}$ stands for the triple summation over n_1, n_2 and n_3, with the above defined limits. The same holds for $\sum_{k_{1,2,3}}$ and $\sum_{m_{1,2,3}}$.

For the sake of brevity, we will henceforth introduce a shorthand notation for the Dirac delta, i.e., Dirac delta $\delta(i_1+i_2+\cdots+i_p-j_1-j_2-\cdots-j_q)$ will be abbreviated as $\delta^{i_1,i_2,\cdots,i_p}_{j_1,j_2,\cdots,j_q}$, where the arguments with the plus sign are listed in the superscript, whereas the arguments with the minus sign (if any) are listed in the subscript. Using this notation and the same reasoning as in (23), the first component of $E[d^3]$ can be calculated according to

$$\begin{aligned}&E[p(i_1+j_1)p(i_1)p(i_2+j_2)p(i_2)p(i_3+j_3)p(i_3)] \\ &= \delta^{j_1}\delta^{j_2}\delta^{j_3} + \delta^{j_1}\delta^{j_2}_{j_3}\delta^{i_2}_{i_3} + \delta^{j_1}\delta^{i_2,j_2}_{i_3}\delta^{i_3,j_3}_{i_2} \\ &+ \delta^{i_1,j_1}_{i_2,j_2}\delta^{i_1}_{i_2}\delta^{j_3} + \delta^{i_1,j_1}_{i_2,j_2}\delta^{i_3,j_3}_{i_1}\delta^{i_2}_{i_3} + \delta^{i_1,j_1}_{i_2,j_2}\delta^{i_3,j_3}_{i_2}\delta^{i_1}_{i_3} \\ &+ \delta^{i_1,j_1}_{i_2}\delta^{i_2,j_2}_{i_1}\delta^{j_3} + \delta^{i_1,j_1}_{i_2}\delta^{i_3,j_3}_{i_1}\delta^{i_2,j_2}_{i_3} \\ &+ \delta^{i_1,j_1}_{i_2}\delta^{i_2,j_2}_{i_3,j_3}\delta^{i_1}_{i_3} + \delta^{i_1,j_1}_{i_3,j_3}\delta^{i_2,j_2}_{i_1}\delta^{i_2}_{i_3} + \delta^{i_1,j_1}_{i_3,j_3}\delta^{i_2,j_2}_{i_3}\delta^{i_1}_{i_2} \\ &+ \delta^{i_1,j_1}_{i_3,j_3}\delta^{i_1}_{i_3}\delta^{j_2} + \delta^{i_1,j_1}_{i_3}\delta^{i_2,j_2}_{i_1}\delta^{i_3,j_3}_{i_2} + \delta^{i_1,j_1}_{i_3}\delta^{i_3,j_3}_{i_2,j_2}\delta^{i_1}_{i_2} \\ &+ \delta^{i_1,j_1}_{i_3}\delta^{i_3,j_3}_{i_1}\delta^{j_2}\end{aligned}$$

$$
\begin{aligned}
&- 2(\delta^{j_1}\delta^{j_2}\delta^{j_3}\delta^{i_1}_{i_2} + \delta^{j_1}\delta^{i_2}_{i_3}\delta^{i_3,j_3}_{i_1}\delta^{i_2,j_2}_{i_1} \\
&+ \delta^{j_1}\delta^{j_2,j_3}\delta^{i_1}_{i_3}\delta^{i_2,j_2}_{i_3} + \delta^{j_1}\delta^{j_2,j_3}\delta^{i_1}_{i_2}\delta^{i_3,j_3}_{i_2} \\
&+ \delta^{j_1}\delta^{j_2}_{j_3}\delta^{i_1}_{i_2}\delta^{i_1}_{i_3} + \delta^{j_1}\delta^{j_2}\delta^{j_3}\delta^{i_1}_{i_3} + \delta^{j_2}\delta^{j_1}_{j_3}\delta^{i_1}_{i_3}\delta^{i_3,j_3}_{i_2} \\
&+ \delta^{j_2}\delta^{j_1,j_3}\delta^{i_2}_{i_3}\delta^{i_3,j_3}_{i_1} + \delta^{j_3}\delta^{j_1}_{j_2}\delta^{i_1}_{i_2}\delta^{i_2,j_2}_{i_3} \\
&+ \delta^{j_3}\delta^{j_1,j_2}\delta^{i_2}_{i_3}\delta^{i_2,j_2}_{i_1} + \delta^{j_2}\delta^{j_1,j_3}\delta^{i_1}_{i_2}\delta^{i_1,j_1}_{i_3} \\
&+ \delta^{j_2}\delta^{j_1}_{j_3}\delta^{i_1}_{i_2}\delta^{i_1}_{i_3} + \delta^{j_3}\delta^{j_1,j_2}\delta^{i_1}_{i_3}\delta^{i_1,j_1}_{i_2} + \delta^{j_3}\delta^{j_1}_{j_2}\delta^{i_1}_{i_2}\delta^{i_1}_{i_3} \\
&+ \delta^{j_1}\delta^{j_2}\delta^{j_3}\delta^{i_2}_{i_3}) + 16\delta^{j_1}\delta^{j_2}\delta^{j_3}\delta^{i_1}_{i_2}\delta^{i_1}_{i_3}.
\end{aligned}
\tag{28}
$$

Substitution of (23) and (28) into (27), and, in turn, (27) back into the definition of μ_3, yields the final expression for μ_3. After straightforward yet tedious calculations, we obtain

$$\mu_3 = \langle \mathbf{W_2}, \mathbf{A} \rangle + 16 \langle \mathbf{x_2}, \mathbf{x_3} \rangle - 6 \langle \mathbf{w_1}, \mathbf{x_4} \rangle \tag{29}$$

where $\mathbf{W_2}$ and $\mathbf{A}$ are the $N \times N$ matrices given by

$$
\begin{aligned}
W_2(m_1, m_2) &= w(m_1)w(m_2)w(m_1+m_2) \\
A(m_1, m_2) &= 2\sum_n [3(1+\sigma_\xi^2) \\
&\quad \times b_{n+m_2}(m_1)b_n(m_1+m_2)b_n(m_2) \\
&\quad + b_n(m_1)b_{n+m_1}(m_2)b_{n+m_1+m_2}(-m_1-m_2)]
\end{aligned}
$$

and $\mathbf{x_3}$ and $\mathbf{x_4}$ are the $1 \times N$ vectors defined as

$$
\begin{aligned}
\mathbf{x_3} &= [b_1^2(0), b_2^2(0), \cdots, b_N^2(0)] \\
x_4(m) &= \sum_n b_n(m) \{b_{n+m}(0) \\
&\quad \times [2b_{n+m}(-m) + b_n(m)] \\
&\quad + (1+\sigma_\xi^2) b_n(0) b_n(m)\}.
\end{aligned}
$$

The validity of (29) is numerically verified in the following section.

Although derived for the jammer excision purpose, the analytical expressions for μ, σ^2 and μ_3 hold not only for binary masks, but for any modification mask $\mathbf{B}$, assuming that the influence of all components, except for the SS and the AWGN, to the decision variable can be neglected in the analysis. In addition, μ and σ^2 have already been derived in matrix form in [6] seeing that the STFT is the special case of the LPFT.

IV. Simulations

A. Jammer is not present

We first consider the case when the received signal does not contain a jammer. The STFT of the received signal, characterized by SNR $= -8$dB, is modified by two types of binary masks, one that excises horizontal bands in the t-f plane and the other that excises diagonal bands. The width of both bands increases from 1 to 14 in increments of 1. Horizontal bands start with the central frequency of the STFT spectrum and then one adjacent upper frequency is added, then one lower, one upper etc. Diagonal bands start with the line that spans one half of the spectrum (that is, starts at $f(1) = \frac{f_{max}}{4}$ and ends at $f(N) = \frac{3f_{max}}{4}$, where $f(n)$ represents the instantaneous frequency (IF) function and f_{max} is the maximal frequency of the spectrum) and then one adjacent upper diagonal is added, one lower, one upper etc. The BEP curves for both excision cases are depicted in Fig. 2(a) and (b). In addition, the BEP versus SNR curves for three fixed band widths, 2, 6 and 10, are depicted in Fig. 2(c) and (d). Clearly, when the excised t-f area is small, the GA still performs satisfactorily, whereas for bigger excised areas it is outperformed by the HGA. The similarity of the results obtained for the two excision cases is due to the fact that both the SS signal and the AWGN are uniformly distributed in the t-f plane. The analysis window used in the STFT calculation is the Kaiser window with the length of 63 samples and $\beta = 10$.

B. Jammer is present

We continue with the case when the received signal is corrupted by various jammer types. Five phase functions $\varphi(n)$, defined in Table I, are considered. Types 1, 2 and 3 respectively correspond to a tone, linear FM (LFM) and quadratic FM jammer, whereas types 4 and 5 respectively conform to the exponential and sinusoidal FM (SFM) model. In addition, a strong impulse jammer, type 6, is also taken into account. It corrupts a segment of five successive chips in the middle of interval. Multicomponent jammers, obtained by combining the introduced jammer types, are also con-

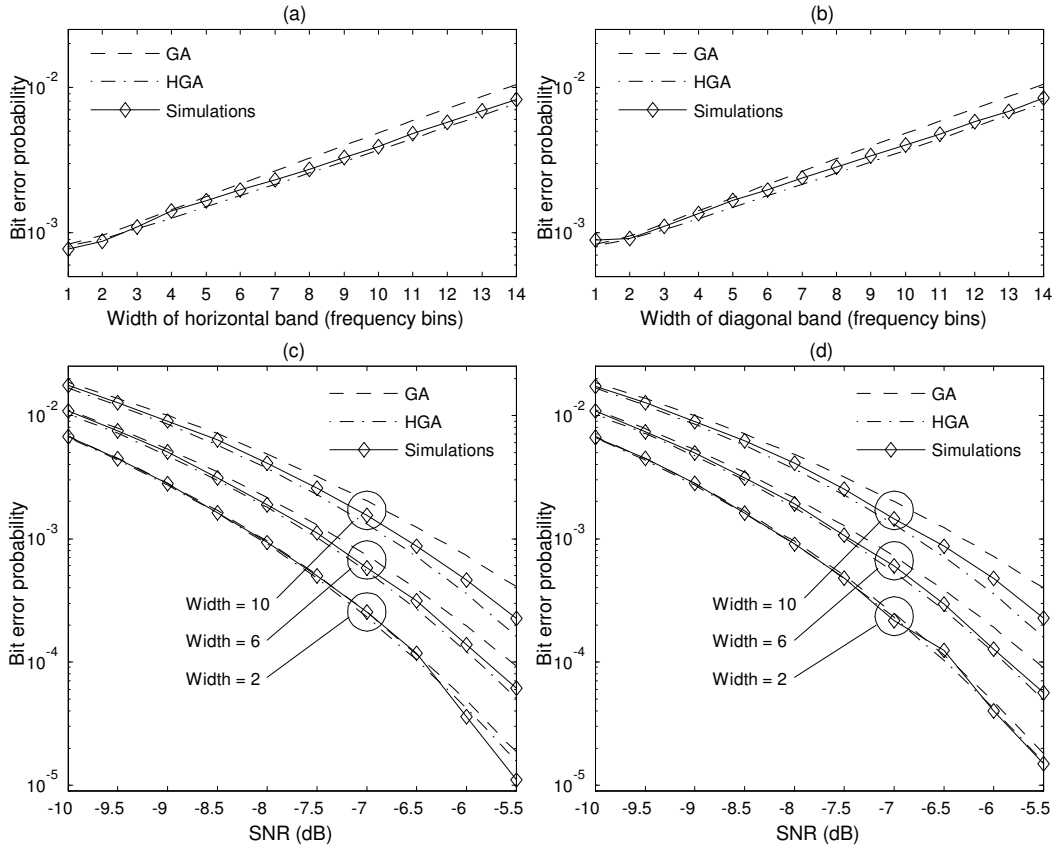

Fig. 2. *Up*: Bit error probability versus the band width for (a) horizontal bands excision and (b) diagonal bands excision. *Down*: Bit error probability versus the SNR for (c) three fixed horizontal band widths and (d) three fixed diagonal band widths.

sidered. In particular, three two-component combinations are herein considered, i.e., combination of types 1 and 3, 2 and 4, as well as 1 and 5. The adopted value for the PN sequence length is $L = 63$, JSR = 20dB and SNR = -7dB. The analysis window used in the STFT calculation is the Kaiser window, whose length is determined according to (9) and additionally zero-padded to 63 samples. The selected value of β for this window is 10^2.

It should be acknowledged that, for each considered jammer, the excision matrix $\mathbf{B}$ is not determined for each run separately, but only for one realization of the STFT of the corrupted received signal [6].

All the obtained analytical and simulated P_e, σ^2 and μ_3 values are presented in Table II, where the first six rows correspond to the monocomponent jammer types 1-6, whereas the last three rows correspond to the multicomponent jammers. The P_e part of Table II clearly indicates that the HGA outperforms the GA for all the considered jammers, with the exception of the impulse jammer when they produce the same results. For the impulse jammer case, the concentration measure yielded a very short analysis window which, in turn, resulted in a binary mask that excises all the frequency bins that correspond to the corrupted and several adjacent chips.

[2]The selection of β is dictated by two conflicting requirements, high sidelobes suppression and narrow main lobe. A small value of β implies narrower main lobe but higher sidelobes, and vice versa. Since the jammer suppression is of primary concern in this paper, we will adopt a bigger value for β at the expense of wider excised area in the t-f plane.

The spectral content of other chips remained intact. Therefore, the decision variable still behaves in accordance with the Gaussian law, which is also supported by the zero analytical value for μ_3. The mean and variance of such a variable are, however, decreased proportionately to the number of excised chips, and (13) still holds.

The σ^2 part of Table II supports the assumption that the residual jammer can be neglected in the analysis since, in all the cases, the difference between the analytically obtained variance and numerical one (which incorporates the influence of the residual jammer) is very small. The last two columns of Table II confirm the validity of (29), while the constantly positive values of μ_3 (except for the impulse jammer), for the adopted SNR value, indicate that the p.d.f. $f_d(x)$ is characterized by longer right tail, implying that the mass of the distribution is concentrated in the region $x > \mu$ [12].

Finally, we consider two jammer types, LFM and SFM jammer, with variable parameters. We changed the modulation index (chirp rate) of the LFM jammer from 0 (a pure sinusoid in the middle of the spectrum) to the value at which its IF sweeps around 65% of the spectrum. Similarly, we changed the amplitude of the IF variation of the SFM jammer from 0 (a pure sinusoid in the middle of the spectrum) to the value at which its IF also sweeps around 65% of the spectrum. The other SFM jammer parameter, the frequency of the IF variation, is the same as for the fifth jammer type from Table I. In addition, $L = 63$, JSR = 20dB and SNR = -7dB. The obtained BEP curves, shown in Fig. 3, indicate that for smaller nonstationarity index the GA performs satisfactorily. However, the excised area increases as the nonstationarity index increases, and the HGA offers better BEP approximation. Note also that the BEP curves of the SFM jammer would rise faster if the frequency of its IF variation was higher and vice versa.

In this section, all the simulated values are obtained over 1 million realizations of the decision variable d.

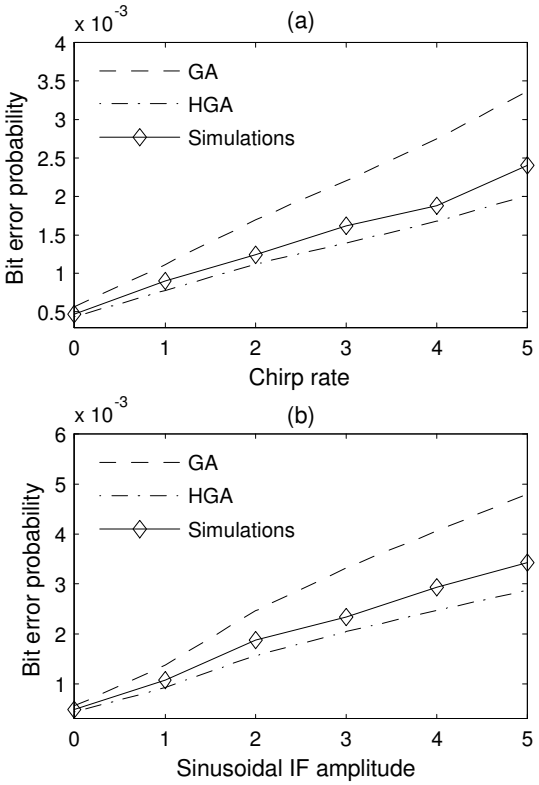

Fig. 3. Bit error probability versus (a) chirp rate of the LFM jammer and (b) amplitude of the IF variation of the SFM jammer.

V. Conclusions

This paper treats the problem of bit error probability approximation in DS-SS systems that implement the STFT as a means of nonstationary jammer excision. The jammer is optimally concentrated in the t-f plane by using the appropriate concentration measure and successively suppressed by removing its t-f signature via a binary mask. Two analytical approximations to the p.d.f. of the decision variable d are proposed, namely the Gaussian approximation (GA) and the Hermite-Gaussian approximation (HGA). The approximation error introduced by the GA is reduced by the HGA, which utilizes the Hermite polynomials and the third central moment of d. Analytical expressions for the mean μ, the variance σ^2 and the third central moment μ_3 of d are derived and numerically confirmed. The HGA outperforms the GA for various types

TABLE I
CONSIDERED JAMMER TYPES

	Jammer's phase
Type 1	$\varphi(n) = 2\pi\frac{n}{3}$
Type 2	$\varphi(n) = 2\pi(\frac{3n}{8} - \frac{n^2}{8N})$
Type 3	$\varphi(n) = 2\pi(\frac{n}{5} - \frac{5n^2}{16N} + \frac{n^3}{4N^2})$
Type 4	$\varphi(n) = 2\pi\frac{3}{\ln(3N/8)}(\frac{3N}{8})^{\frac{2}{3}}e^{\frac{\ln(3N/8)}{3N}n}$
Type 5	$\varphi(n) = 2\pi\left[\frac{N}{10\pi}\cos(\frac{5\pi}{4N}n + \frac{\pi}{4}) + \frac{n}{4}\right]$
Type 6	Impulse jammer

TABLE II
ANALYTIC AND SIMULATED VALUES OF P_e, σ^2 AND μ_3

	Bit Error Probability P_e			Variance σ^2		Moment μ_3	
	GA	HGA	Simul.	Analytic	Simul.	Analytic	Simul.
Type 1	5.611e-4	4.369e-4	4.640e-4	264.646	265.825	168.822	160.006
Type 2	2.802e-3	1.710e-3	1.992e-3	198.211	199.651	318.550	305.635
Type 3	4.826e-3	3.066e-3	3.513e-3	178.113	180.748	314.546	303.893
Type 4	2.663e-3	1.660e-3	1.936e-3	203.591	206.721	314.515	318.115
Type 5	3.428e-3	2.127e-3	2.529e-3	193.748	197.047	323.369	328.385
Type 6	4.149e-4	4.149e-4	3.980e-4	280.665	280.462	0	-10.211
Type 1+Type 3	1.359e-2	8.291e-3	9.640e-3	108.275	111.591	265.606	262.637
Type 2+Type 4	1.161e-2	7.324e-3	8.471e-3	125.352	128.581	286.408	298.498
Type 1+Type 5	7.668e-3	4.642e-3	5.729e-3	145.604	148.668	309.713	321.588

of monocomponent and multicomponent jammers, which was verified by simulations. However, the GA performs satisfactorily when the excised t-f area is small.

The analytical expressions for μ, σ^2 and μ_3 are valid for any modification mask $\mathbf{B}$ (i.e., not only binary) given that the contribution of all components, apart from the SS and the AWGN, to the decision variable can be neglected.

The similar treatment can be carried out when the synthesis is performed via the OLA method which incorporates one summation more compared to the synthesis method used herein.

REFERENCES

[1] M.G. Amin, Interference mitigation in spread spectrum communication systems using time-frequency distributions, IEEE Trans. Signal Process. 45 (1) (1997) 90–101.

[2] B. Boashash, Time-frequency signal analysis and processing, Elsevier, 2003, Chapters 2 and 4.

[3] X. Ouyang and M.G. Amin, Short-time Fourier transform receiver for nonstationary interference excision in direct sequence spread spectrum communications, IEEE Trans. Signal Process. 49 (4) (2001) 851-863.

[4] O. Akay and G.F. Boudreaux-Bartels, Broadband interference excision in spread spectrum communication systems via fractional Fourier transform, Proc. Asilomar Conf. on Sig., Sys. and Comp., November 1998, pp. 832-837.

[5] Lj. Stanković and S. Djukanović, Order adaptive local polynomial FT based interference rejection in spread spectrum communication systems, IEEE Trans. Instrumentat. Meas. 54 (12) (2005) 2156-2162.

[6] S. Djukanović, M. Daković and Lj. Stanković, Local polynomial Fourier transform receiver for nonstationary interference excision in DSSS communications, IEEE Trans. Signal Process. 56 (4) (2008) 1627-1636.

[7] Lj. Stanković, A measure of some time-frequency distributions concentration, Signal Processing, 81 (3) (2001) 621-631.

[8] J.A. Young and J.S. Lehnert, Analysis of DFT-based frequency excision algorithms for direct-sequence spread-spectrum communications, IEEE Trans. Commun. 46 (8) (1998) 1076-1087.

[9] B.Q. Long, J.D. Hu and P. Zhang, Method to improve Gaussian approximation accuracy for calculation of spread-spectrum multiple-access error

probabilities, IEE Electron. Letters 31 (3) (1995) 529–531.
[10] G.L. Stüber, Principles of Mobile Communications, Kluwer Academic Publishers, Massachusetts-USA, 2001, Chapter 9, pp. 459-462.
[11] R.L. Pickholtz, D.L. Schilling and L.B. Milstein, Theory of spread-spectrum communications - A tutorial, IEEE Trans. Commun. COM-30 (5) (1982) 855-884.
[12] A. Papoulis, Probability, random variables, and stochastic processes, 3rd edition, McGraw-Hill, New York, 1991, Chapters 4 and 8.
[13] R.N. McDonough and A.D. Whalen, Detection of Signals in Noise, 2nd edition, Academic Press, San Diego, 1995, Chapters 5 and 8.